Received: 30 September 2022 | Revised: 5 April 2023 | Accepted: 10 May 2023

DOI: 10.1002/mp.16528

RESEARCH ARTICLE

MEDICAL PHYSICS

Averaging of absorbed doses: How matter matters

Johan Gustafsson[1] | **Michael Ljungberg**[1] | **Gudrun Alm Carlsson**[2] | **Erik Larsson**[3] | **Carl Fredrik Warfvinge**[4] | **Pernilla Asp**[4] | **Katarina Sjögreen Gleisner**[1]

[1]Medical Radiation Physics, Lund, Lund University, Lund, Sweden

[2]Department of Radiation Physics, Faculty of Health Sciences, Linköping University, Linköping, Sweden

[3]Radiation Physics, Skåne University Hospital, Lund, Sweden

[4]Division of Oncology and Pathology, Department of Clinical Sciences Lund, Lund University, Lund, Sweden

Correspondence
Gustafsson Johan, Medical Radiation Physics, Lund, Lund University, Lund, Sweden.
Email: johan_ruben.gustafsson@med.lu.se

Funding information
Swedish Cancer Society, Grant/Award Numbers: 180747, 211754Pj01H; Mrs. Berta Kamprad's Foundation, Grant/Award Numbers: FBKS 2019-44, FBKS-2020-13-293

Abstract

Background: Dosimetry in radionuclide therapy often requires the calculation of average absorbed doses within and between spatial regions, for example, for voxel-based dosimetry methods, for paired organs, or across multiple tumors. Formation of such averages can be made in different ways, starting from different definitions.

Purpose: The aim of this study is to formally specify different averaging strategies for absorbed doses, and to compare their results when applied to absorbed dose distributions that are non-uniform within and between regions.

Methods: For averaging within regions, two definitions of the average absorbed dose are considered: the simple average over the region (the region average) and the average when weighting by the mass density (density-weighted region average). The latter is shown to follow from the definition of mean absorbed dose according to the ICRU, and to be consistent with the MIRD formalism. For averaging between different spatial regions, three definitions follow: the volume-weighted, the mass-weighted, and the unweighted average. With respect to characterizing non-uniformity, the different average definitions lead to the use of dose-volume histograms (DVHs) (region average), dose-mass histograms (DMHs) (density-weighted region average), and unweighted histograms (unweighted average). Average absorbed doses are calculated for three worked examples, starting from the different definitions. The first, schematic, example concerns the calculation of the average absorbed dose between two regions with different volumes or mass densities. The second, stylized, example concerns voxel-based dosimetry, for which the average absorbed-dose rate within a region is calculated. The geometries studied include three ^{177}Lu-filled voxelized spheres, where the sphere masses are held constant while the material compositions, densities, and volumes are varied. For comparison, the mean absorbed-dose rates obtained using unit-density sphere S-values are also included. The third example concerns SPECT/CT-based tumor dosimetry for five patients undergoing therapy with ^{177}Lu-PSMA and six patients undergoing therapy with ^{177}Lu-DOTA-TATE, for which the average absorbed-dose rates across multiple tumors are calculated. For the second and third examples, analyses also include representations by histograms.

Results: Example 1 shows that the average absorbed doses, calculated using different definitions, can differ considerably if the masses and absorbed doses for two regions are markedly different. From example 2 it is seen that the density-weighted region average is stable under different activity and density distributions and is also in line with results using S-values. In contrast, the region

average varies as function of the activity distribution. In example 3, the absorbed dose rates for individual tumors differ by (1.1 ± 4.3)% and (−0.1 ± 0.4)% with maximum deviations of +34.4% and −1.4% for ^{177}Lu-PSMA and ^{177}Lu-DOTATATE, respectively, when calculated as region averages or density-weighted region averages, with largest deviations obtained when the density is non-uniform. The average absorbed doses calculated across all tumors are similar when comparing mass-weighted and volume-weighted averages but these differ substantially from unweighted averages.

Conclusion: Different strategies for averaging of absorbed doses within and between regions can lead to substantially different absorbed-dose estimates. At reporting of radionuclide therapy dosimetry, it is important to specify the averaging strategy applied.

KEYWORDS
average absorbed dose, dose-mass histogram, dose-volume histogram, dosimetry, radionuclide therapy

1 | INTRODUCTION

The radiotherapeutic modality radionuclide therapy currently undergoes an expansion with new radiopharmaceuticals being developed and introduced for an increasing number of treatment indications. Dosimetry leads to an improved understanding of how the radiotherapy is delivered and can contribute to optimization of the treatment both at the group level and for the individual patient.[1] The expanding use of radionuclide therapy, combined with an increased clinical availability of quantitative SPECT, has led to an increasing number of reports of absorbed doses for both tumors and risk organs, with the ultimate aim of deriving relationships of absorbed doses with patient outcome.[2–7] The dosimetry methods used range from simpler whole-organ-based methods to more complex voxel-wise calculations. Several studies also focus on method development or method comparison.[8–13]

Recently, three major guidance documents on patient-specific dosimetry in radionuclide therapy have been issued.[14–16] However, there is yet no formal code-of-practice for how dosimetry in radionuclide therapy should be performed or methods validated. Consequently, there is a risk that method comparisons give misleading results. In particular, we have identified inconsistencies when comparing absorbed doses calculated by averaging across voxels or across multiple, anatomically separate regions. Our aim is here to demonstrate the need of specifying how average absorbed doses are calculated, both when comparing results of different dosimetry methods, and for reporting and recording.

Generally, dosimetry in radiotherapy can be separated into two sub-tasks: (1) characterization of the radiation source and (2) calculation of the radiation transport from the source to the target and energy deposition in different tissues. In radionuclide therapy, the uncertainty in absorbed dose estimates is typically dominated by the uncertainty in the characterization of the radiation source.[17,18] However, there is also interest in examining different methods for calculating the radiation transport, in particular the consequences of the spatial scale at which the absorbed dose is calculated. Historically, dosimetry has been performed with the aim of determining the mean absorbed dose to whole organs. Such calculations have been formalized through the MIRD formalism[19] and there are several tools available to support its application.[20–22] In parallel, there is an ambition to calculate absorbed doses at the voxel level,[23] to better account for the detailed patient-specific geometric and physical properties and to describe the distribution of absorbed doses, typically in the form of dose-volume histograms (DVHs).[24] Voxel-based dosimetry can be accomplished from a series of SPECT/CT images, with the patient specific source-distribution derived from the SPECT image, and the radiation transport calculated in the CT-derived geometry.[25,26] Different voxel-based calculation algorithms are available,[9,27] with direct Monte Carlo simulations typically considered to be the most accurate but suffering from a relatively high complexity and computational burden.

Practically, when applying voxel-based methods for patient dosimetry, there is often the need to aggregate the voxel-wise absorbed doses into averages across entire organs or tumors for recording and reporting. Averaging is also required when reporting aggregated values for functionally connected, but anatomically separated, regions such as the right and left kidney.[28] Another example of averaging is for estimation of the mean absorbed dose across multiple lesions,[29] for which the absorbed doses are expected vary due to both variable activity uptakes and densities, such as for bone and soft tissue. In these cases, averaging is applied to simplify a large data set into an interpretable scalar. A related issue is the limited spatial resolution of SPECT images, which leads to the need for compensation for the resolution-induced error of estimated activity concentrations. Correction

for these so-called partial-volume effects is typically implemented at the region level,[30] in the simplest case by applying recovery coefficients. Thus, absorbed doses for functionally related, but anatomically separate, regions must first be calculated individually, and then averaged.

Thus, the quantity mean absorbed dose is central for radionuclide therapy dosimetry, and in practice there is a need to aggregate absorbed doses, calculated at different spatial scales, into averages across voxels or multiple regions. The scale over which such averages are formed are governed by: (1) the purpose of the dosimetry and the constitution of the target region, which can be an organ, a paired organ, or one or several lesions, (2) the technique used to characterize the source distribution (usually SPECT) and its spatial resolution, and (3) the technique used to characterize the distribution of matter (usually CT).

At first glance, averaging may seem like a simple operation, but it turns out that it is not obvious how these averages should be formed. The purpose of this study is to specify different versions of averaging of absorbed doses and compare these from a physical perspective. The average versions represent the different definitions found in the literature of radionuclide therapy dosimetry. The formulae are derived from formal definitions and applied to examples of averages both across voxels and between multiple regions. From the definitions, the corresponding absorbed-dose histograms are derived and examined for illustrative examples.

2 | THEORY

2.1 | Definitions

The description starts in continuous space and then transitions to discrete space, treated as an approximation of the continuous case. Terminology-wise, *volume* will refer to the integral of the unity function over a region Ω in three-dimensional space, $V = \int\int\int_{\Omega} \mathrm{d}x\mathrm{d}y\mathrm{d}z$, as illustrated in Figure 1. According to commonly used terminology, a region in three-dimensional space is often referred to as a "volume." However, this means that the same term is used to denote the spatial region and its measure.[14] Since the concept of volume, in the sense of the measure of a set of points in three-dimensional space, is central to this study, we find it important to distinguish between a region and the volume of that region. For the discrete case, we adhere to the term *volume-of-interest* (VOI) to denote the set of logical units in an image (voxels) selected to represent the region Ω.

Absorbed dose is defined as[31]

$$D\ (x, y, z) = \frac{\mathrm{d}\bar{\varepsilon}}{\mathrm{d}m} \tag{1}$$

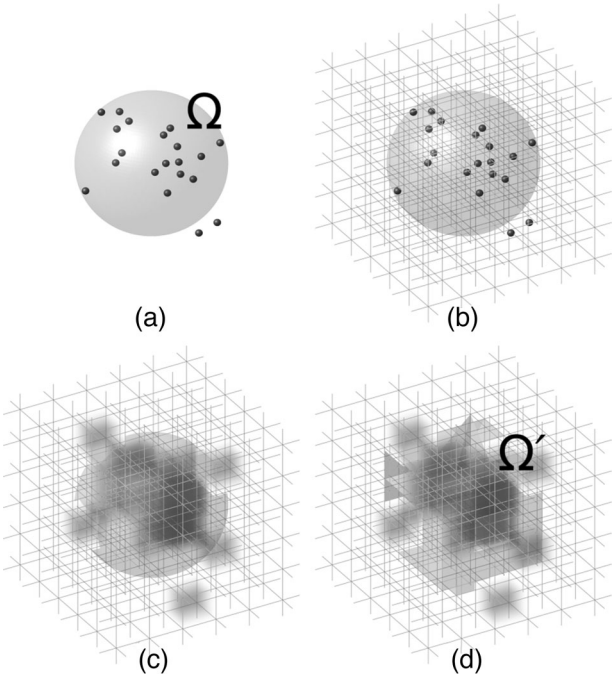

FIGURE 1 Illustration of the transition from continuous to discrete space. (a) Energy is deposited to matter in three-dimensional space, some of which is within the region Ω with volume V and mass M. (b) Space is considered to consist of a set of cuboid regions. (c) Absorbed dose is approximated using the basis functions in Equations (7) and (8). (d) The region Ω is approximated with a set of cuboid regions Ω'.

which is to be interpreted as the ratio between the expected energy imparted to a mass element and the mass of that element, at the limit of an infinitesimal spatial extent. Through the formation of the limit, the absorbed dose is associated with a point, designated (x, y, z), and the absorbed dose is thus a quantity that varies pointwise in space.

In practice, it is rarely possible to measure or calculate the absorbed dose in the sense that it is associated with a point, but the deposited energy is associated with a spatial region of volume V and mass M. Technically, the quantity is then a *mean absorbed dose*, as opposed to the point-wise quantity in Equation (1). Mathematically, the mean absorbed dose $\bar{D}$ is defined as[32]

$$\bar{D} = \frac{\iiint_{\Omega} D\,(x, y, z) \cdot \rho\,(x, y, z)\ \mathrm{d}x\mathrm{d}y\mathrm{d}z}{\iiint_{\Omega} \rho\,(x, y, z)\ \mathrm{d}x\mathrm{d}y\mathrm{d}z} = \frac{\bar{\varepsilon}}{M} \tag{2}$$

where Ω is the spatial region over which the mean is calculated, $\rho(x, y, z)$ is the spatially varying density, and $\bar{\varepsilon}$ is the absorbed energy in the region. The mean absorbed dose is thus defined as the absorbed energy divided by the mass of the region and is obtained by weighting the point-wise absorbed doses with the density when forming the average over Ω. This average will henceforth be referred to as a *density-weighted region-average*.

In contrast to Equation (2), an average on the form

$$\bar{D}_{\mathrm{r}} = \frac{\iiint_{\Omega} D(x,y,z)\ \mathrm{d}x\mathrm{d}y\mathrm{d}z}{\iiint_{\Omega} \mathrm{d}x\mathrm{d}y\mathrm{d}z} \tag{3}$$

is often used. Since this average is formed unweighted over the region it will simply be referred to as a *region-average*. The region-average coincides with the density-weighted region-average if the density is uniform within Ω.

2.2 | Averaging between regions

Assume n non-overlapping regions ω_q, $q = 1 \ldots n$, in the sense that the volume of $\omega_i \cap \omega_j$ is 0 if $i \neq j$. Following Equation (2), the density-weighted region-average over the union of the n regions, $\cup_{q=1}^{n} \omega_q$, becomes

$$\begin{aligned}\bar{D} &= \frac{\iiint_{\cup_{q=1}^{n}\omega_q} D(x,y,z)\,\rho(x,y,z)\,\mathrm{d}x\mathrm{d}y\mathrm{d}z}{\iiint_{\cup_{q=1}^{n}\omega_q} \rho(x,y,z)\,\mathrm{d}x\mathrm{d}y\mathrm{d}z} \\ &= \frac{\sum_{q=1}^{n} \iiint_{\omega_q} D(x,y,z)\ \rho(x,y,z)\ \mathrm{d}x\,\mathrm{d}y\,\mathrm{d}z}{\sum_{q=1}^{n} \iiint_{\omega_q} \rho(x,y,z)\ \mathrm{d}x\,\mathrm{d}y\,\mathrm{d}z} \\ &= \frac{\sum_{q=1}^{n} \bar{D}_q m_q}{\sum_{q=1}^{n} m_q} = \frac{\sum_{q=1}^{n} \bar{\varepsilon}_q}{\sum_{q=1}^{n} m_q},\end{aligned} \tag{4}$$

where $\bar{D}_q$ is the mean absorbed dose to region q with mass m_q, and $\bar{\varepsilon}_q$ is the absorbed energy in region q. Thus, the mean absorbed dose to, for example, a group of tumors is given by the mass-weighted average of the mean absorbed doses (Equation 2) to the individual entities, or, equivalently, the total absorbed energy to all tumors divided by the total mass of all tumors.

Following Equation (3), the region-average over the union of the regions is given by

$$\begin{aligned}\bar{D}_{\mathrm{r}} &= \frac{\iiint_{\cup_{q=1}^{n}\omega_q} D(x,y,z)\ \mathrm{d}x\,\mathrm{d}y\,\mathrm{d}z}{\iiint_{\cup_{q=1}^{n}\omega_q} \mathrm{d}x\,\mathrm{d}y\,\mathrm{d}z} \\ &= \frac{\sum_{q=1}^{n} \iiint_{\omega_q} D(x,y,z)\,\mathrm{d}x\,\mathrm{d}y\,\mathrm{d}z}{\sum_{q=1}^{n} \iiint_{\omega_q} \mathrm{d}x\,\mathrm{d}y\,\mathrm{d}z} \\ &= \frac{\sum_{q=1}^{n} \bar{D}_{\mathrm{r},q}\ v_q}{\sum_{q=1}^{n} v_q},\end{aligned} \tag{5}$$

where $\bar{D}_{\mathrm{r},q}$ is the region-average of the absorbed dose to region q with volume v_q. The region-average of the absorbed doses to the union of the regions is thus obtained as the volume-weighted average of the region-averages for the individual regions.

TABLE 1 The relationship between different definitions for calculating average absorbed doses across multiple regions. The table specifies situations when different definitions coincide, depending on how the density and volume vary between the individual regions.

Average within one region	
Uniform density	Density-weighted region-average (Equation 2) = region-average (Equation 3)
Average across regions	
Same density for all regions	Density-weighted region-average (Equation 4) = region-average (Equation 5)
Same volume for all regions	Region-average (Equation 5) = unweighted average (Equation 6)
Same density and volume for all regions	Density-weighted region-average (Equation 4) = region-average (Equation 5) = unweighted-average (Equation 6)

Furthermore, an unweighted average of absorbed doses is often used. This can be calculated for both density-weighted region-averages (Equation 2) and region-averages (Equation 3), according to

$$\bar{D}_{\mathrm{u}} = \frac{\sum_{q=1}^{n} \bar{D}'_q}{n}, \tag{6}$$

where $\bar{D}'_q$ denotes either $\bar{D}_q$ (as in Equation 4) or $\bar{D}_{\mathrm{r},q}$ (as in Equation 5). This average has no direct physical interpretation and is referred to as the *unweighted average* of the respective quantity.

Thus, there are different ways to calculate the average absorbed dose between regions. The physical quantity mean absorbed dose leads to the density-weighted region-average (Equation 4), but in practical applications region-averages (Equation 5) or unweighted averages (Equation 6) are often used. For example, it is common to report absorbed doses to kidneys in peptide receptor radionuclide therapy as the unweighted average of the absorbed dose to the right and left kidneys, often without explicitly stating how this average was formed. Under certain conditions, the different definitions coincide, as presented in Table 1.

In practice, different forms of averages may be mixed in the sense that different definitions may be used for averaging within regions and between regions, although some combinations are more logically coherent than others. For example, the density-weighted average within regions (Equation 2) is coherent with a mass-weighted average between regions (Equation 4), while combining simple region averages within regions

(Equation 3) with a mass-weighted average between regions may be considered illogical.

2.3 | Averaging of voxel-wise absorbed doses

Discretization of space can be viewed from different perspectives,[33,34] and the same applies to the interpretation of voxels. One way to interpret the physical meaning of a voxel in a three-dimensional image is to consider the signal distribution $g(x, y, z)$ within the region $\{(x, y, z); 0 \le x < A,\ 0 \le y < B,\ 0 \le z < C\}$ as being well-approximated by a series of basis-functions such that[34]

$$g\ (x, y, z) = \sum_{i=0}^{N_x-1} \sum_{j=0}^{N_y-1} \sum_{k=0}^{N_z-1} g_{ijk} \cdot f_{ijk}\ (x, y, z)\ , \qquad (7)$$

where g_{ijk} is a scalar and

$$f_{ijk}\ (x, y, z) = \begin{cases} 1, & i\Delta x \le x < (i+1)\,\Delta x,\ j\Delta y \le y\,(j+1)\,\Delta y, k\Delta z \le z < (k+1)\,\Delta z \\ 0, & \text{otherwise} \end{cases}, \qquad (8)$$

with $\Delta x = A/N_x, \Delta y = B/N_y$, and $\Delta z = C/N_z$. Using this representation, a voxel (i, j, k) is associated with a cuboid region with volume $\Delta x \Delta y \Delta z$ and value g_{ijk}. The transition from continuous to discrete representation is illustrated in Figure 1.

Following Equation (2), the mean absorbed dose to a set of voxels Ω' is

$$\bar{D} = \frac{\sum_{(i,j,k)\in\Omega'} D_{ijk}\ m_{ijk}}{\sum_{(i,j,k)\in\Omega'}\ m_{ijk}} = \frac{\sum_{(i,j,k)\in\Omega'} D_{ijk}\ \rho_{ijk}}{\sum_{(i,j,k)\in\Omega'}\ \rho_{ijk}}\ , \qquad (9)$$

where D_{ijk} is the absorbed dose to voxel (i, j, k) and ρ_{ijk} is the density of the voxel. Thus, for voxel-based calculations, the mean absorbed dose is obtained as a density-weighted region-average of the absorbed doses to the individual voxels.

The discrete equivalence of Equation (3) for calculating the region-average becomes

$$\bar{D}_{\mathrm{r}} = \frac{\sum_{(i,j,k)\in\Omega'} D_{ijk}\Delta x\Delta y\Delta z}{\sum_{(i,j,k)\in\Omega'} \Delta x\Delta y\Delta z} = \frac{\sum_{(i,j,k)\in\Omega'} D_{ijk}}{|\Omega'|}\ , \qquad (10)$$

where $|\cdot|$ denotes the cardinality of a set, that is, $|\Omega'|$ is the number of voxels in the VOI.

If all voxels in a region have the same density, Equations (9) and (10) coincide. Similarly, if the density variation in a region is low, as is typical for soft tissue, the difference between the averages from Equations (9) and (10) will be small. However, in cases of pronounced density variations, such as for soft tissue mixed with lung or bone, the differences between the two averages can become substantial.

2.4 | Mean absorbed dose according to the MIRD formalism

Using the MIRD formalism, the mean absorbed dose to a target region r_{T} is calculated from the decays in a source region r_{S} according to[19]

$$\bar{D}\ (r_{\mathrm{T}} \leftarrow r_{\mathrm{S}}) = \tilde{A}_{r_{\mathrm{S}}}\ \cdot S\,(r_{\mathrm{T}} \leftarrow r_{\mathrm{S}}) \qquad (11)$$

where $\tilde{A}_{r_{\mathrm{S}}}$ is the time-integrated activity in the source region and the coefficient $S(r_{\mathrm{T}} \leftarrow r_{\mathrm{S}})$ describes the radiation transport and absorption of energy from source to target regions. For a given radionuclide, the S-value is given by

$$S\ (r_{\mathrm{T}} \leftarrow r_{\mathrm{S}}) = \frac{\theta\,(r_{\mathrm{T}} \leftarrow r_{\mathrm{S}})}{m_{\mathrm{T}}} \qquad (12)$$

where $\theta\ (r_{\mathrm{T}} \leftarrow r_{\mathrm{S}}) = \sum_i \Delta_i \varphi_i (r_{\mathrm{T}} \leftarrow r_{\mathrm{S}})$ is the mean absorbed energy in target r_T per time-integrated activity in source r_{s}, and m_{T} is the mass of the target region. Δ_i is the mean energy per time-integrated activity for emitted radiation i and $\varphi_i(r_{\mathrm{T}} \leftarrow r_{\mathrm{S}})$ is the fraction of the energy emitted from r_{S} that is absorbed in r_{T} (absorbed fraction) for radiation i. The mean absorbed dose to r_{T} is obtained as the sum of the contributions from all source regions

$$\begin{aligned} \bar{D}_{r_{\mathrm{T}}} &= \sum\nolimits_{r_{\mathrm{S}}} \tilde{A}_{r_{\mathrm{S}}} \cdot S\,(r_{\mathrm{T}} \leftarrow r_{\mathrm{S}}) \\ &= \sum\nolimits_{r_{\mathrm{S}}} \tilde{A}_{r_{\mathrm{S}}} \cdot \frac{\theta\,(r_{\mathrm{T}} \leftarrow r_{\mathrm{S}})}{m_{\mathrm{T}}} \\ &= \frac{1}{m_{\mathrm{T}}} \sum\nolimits_{r_{\mathrm{S}}} \tilde{A}_{r_{\mathrm{S}}} \cdot \theta\,(r_{\mathrm{T}} \leftarrow r_{\mathrm{S}})\,. \end{aligned} \qquad (13)$$

Since $\sum_{r_{\mathrm{S}}} \tilde{A}_{r_{\mathrm{S}}} \cdot \theta(r_{\mathrm{T}} \leftarrow r_{\mathrm{S}})$ is the absorbed energy in matter in r_{T}, Equations (13) and (2) are consistent. The calculation of the mean absorbed dose according to the MIRD formalism is thus consistent with a density-weighted region-average.

2.5 | Dose-volume histograms and dose-mass histograms

A common way to analyze the distribution of absorbed doses in a region is to use DVHs. Formally, the cumulative DVH can be defined as the fraction of all

points in a region Ω for which the absorbed dose is greater than a given absorbed dose δ. Mathematically this can be formulated as

$$\mathrm{DVH}\ (\delta) = 1 - \frac{1}{V} \iiint_{\{(x,y,z)\in\Omega; D(x,y,z)\le\delta\}} \mathrm{d}x\mathrm{d}y\mathrm{d}z \quad (14)$$

where $D(x, y, z)$ is the distribution of absorbed dose and V is the volume of Ω.

In line with the previous reasoning, from a physical perspective it is more relevant to study the distribution of absorbed dose over matter in the region, rather than over the region itself. This can be performed with so-called dose-mass histograms (DMHs).[35] For the case of DMHs, the fraction of points in the region Ω is weighted by the density of these points, such that

$$\mathrm{DMH}\ (\delta) = 1 - \frac{1}{M} \iiint_{\{(x,y,z)\in\Omega; D(x,y,z)\le\delta\}} \rho\,(x, y, z)\,\mathrm{d}x\mathrm{d}y\mathrm{d}z, \quad (15)$$

where M is the mass of the matter in Ω. Thus, DMH can be seen as a density-weighted variant of DVH, in analogy with the difference between a region average and a density-weighted region average.

2.5.1 | Voxel-based dosimetry

The discrete counterpart of Equation (14) is given by

$$\mathrm{DVH}\ (\delta) = 1 - \frac{1}{|\Omega'|} \sum_{\{(i,j,k)\in\Omega'; D_{ijk}\le\delta\}} 1. \quad (16)$$

For Equation (15), the discrete counterpart becomes

$$\mathrm{DMH}\ (\delta) = 1 - \frac{1}{\sum_{(i,j,k)\in\Omega'} \rho_{ijk}} \sum_{\{(i,j,k)\in\Omega'; D_{ijk}\le\delta\}} \rho_{ijk}. \quad (17)$$

2.5.2 | Region-based dosimetry

DVHs and DMHs can also be constructed across multiple regions with different volumes or masses, which can be useful, for example, when analyzing the absorbed doses delivered to several tumors in a patient. For a total of n sub-regions, the DVH of the mean absorbed doses to the sub-regions, DVH($\bar{\delta}$), is given by

$$\mathrm{DVH}\ (\bar{\delta}) = 1 - \frac{1}{\sum_{j=1}^{n} v_j} \sum_{\{j\in 1,2\ldots n;\ \bar{D}_{\mathrm{r},j} < \bar{\delta}\}} v_j. \quad (18)$$

The region-average absorbed dose, $\bar{D}_{\mathrm{r},j}$, for each subregion is obtained from Equation (5). The DMH($\bar{\delta}$) becomes

$$\mathrm{DMH}\ (\bar{\delta}) = 1 - \frac{1}{\sum_{j=1}^{n} m_j} \sum_{\{j\in 1,2\ldots n;\ \bar{D}_j < \bar{\delta}\}} m_j, \quad (19)$$

The density-weighted region average absorbed dose to the respective sub-region, $\bar{D}_j$, can be calculated by voxel-based (Equation 4) or region-based dosimetry methods, for example by applying S-values according to the MIRD formalism.

As a link to the unweighted average over regions (Equation 6), an unweighted histogram DUH($\bar{\delta}$) can also be formed, following

$$\mathrm{DUH}\ (\bar{\delta}) = 1 - \frac{1}{n} \sum_{\{j\in 1,2\ldots n;\ \bar{D}'_j < \bar{\delta}\}} 1. \quad (20)$$

With this histogram, each of the sub-regions are considered without accounting for their relative volumes or masses. Such an approach may be justified under the assumption that the relative influence of the mean absorbed doses for the sub-regions should not scale with size. For example, it is not obvious that a set of tumors should be prioritized by size if there are other, clinically more relevant, parameters to consider.

3 | MATERIAL AND METHODS

The consequences of different averaging methods for the absorbed dose are illustrated by three examples. For simplicity, two of the examples consider the absorbed-dose rate instead of absorbed dose since the principles for spatial averaging of absorbed dose also applies to absorbed-dose rate.

3.1 | Schematic example

Figure 2 shows two schematic geometries chosen to illustrate averaging between regions. Averaging was performed following Equation (4), to give $\bar{D}$, and with

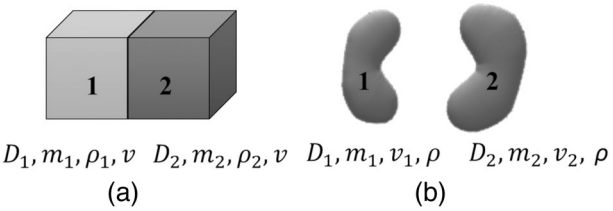

FIGURE 2 (a) Two regions with identical volumes v, but with different densities ρ_1 and ρ_2, masses m_1 and m_2, and absorbed doses D_1 and D_2. (b) Two regions with the same mean density ρ, but with different volumes, masses, and absorbed doses.

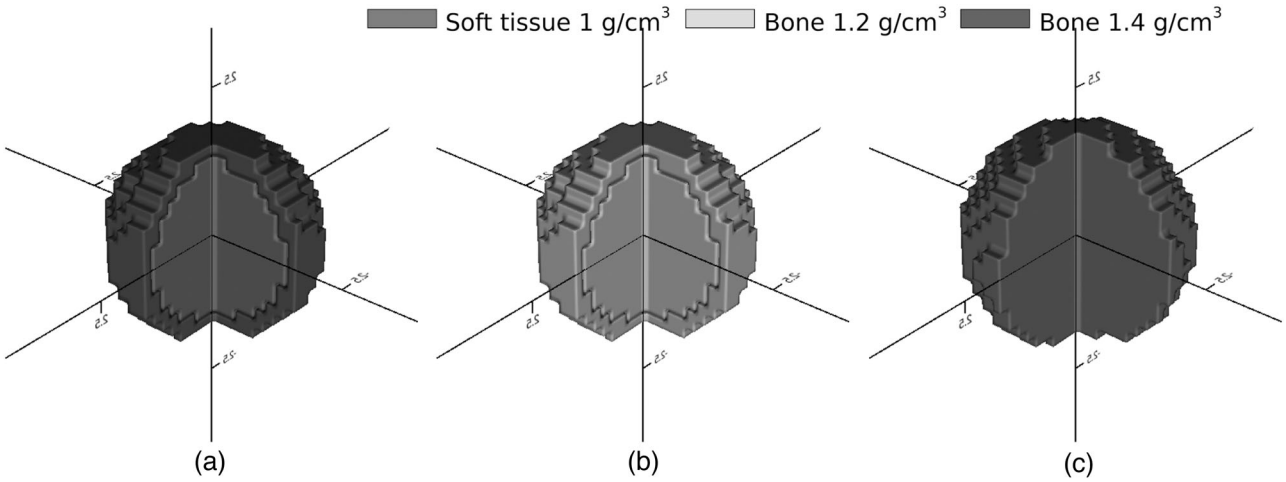

FIGURE 3 The three voxelized sphere geometries (a), (b), and (c) (Table 2) filled with ^{177}Lu.

TABLE 2 Three voxelized sphere geometries, each with a total ^{177}Lu activity of 10 MBq and with different density distributions.

	Sph. vol./mL	Num. of compartm. (compartm. vol./mL)	Material		Dens./(g mL^{-1})		Act. distribution
			Core	Shell	Core	Shell	
a	20	2 (10)	Soft tissue	Bone	1.0	1.4	Non-uniform
b	20	2 (10)	Bone	Bone	1.2	1.2	Non-uniform
c	24	1 (24)	Soft tissue		1.0		Uniform

Equation (6), to give $\bar{D}_u$, both with $n = 2$. The relative difference was calculated as $\bar{D}_u/\bar{D} - 1$. For the geometry in Figure 2a, with identical volumes for the two regions, $\bar{D}_r = \bar{D}_u$ and the relative difference coincides with $\bar{D}_r/\bar{D} - 1$. The explicit expression for the relative difference is given in Appendix A.

3.2 | Averaging for voxel-based dosimetry

Figure 3 shows the geometries chosen to illustrate the effects of averaging between voxels (Equations 9 and 10). These include three voxelized sphere geometries, referred to as *a*, *b*, and *c*, with a distribution of 177Lu. The absorbed-dose rate was calculated using a Monte-Carlo program for voxel-based dosimetry.[36] Originally, this program was based on EGS4, but has since been updated to use EGSnrc[37] as underlying physics engine. The emission spectrum for 177Lu was taken from the LNHB recommended data[38] (www.lnhb.fr/nuclear-data/nuclear-data-table/) and cut-off energies set to 10 keV for both photons and electrons in the simulations. Elemental compositions were taken as Tissue, soft (ICRP) and Bone, cortical (ICRP) from the NIST STAR databases (physics.nist.gov/cgi-bin/Star/compos.pl). The spheres were surrounded by soft tissue with a density of 1.0 g mL−1, and the voxel size was $0.2 \times 0.2 \times 0.2$ cm^3. Table 2 lists the specifications for the three geometries.

The spheres in geometries *a* and *b* had two compartments, an inner core and an outer shell. Monte Carlo simulations were performed separately with activities in cores and shells and the resulting absorbed-dose rate images combined to correspond to total activities of 10 MBq, with variable activity-ratios between the core and the shell. As the core and shell had the same volume, the ratio of the activity concentrations was the same as the ratio of the activities. For geometry *a*, the densities were 1.0 g mL−1 (soft tissue) and 1.4 g mL−1 (bone) for the core and shell, respectively. For geometry *b*, the sphere density was set uniformly to 1.2 g mL−1, that is, the mean density of the sphere in geometry *a*. In this way, the effects of a varied activity distribution were investigated without influence of a non-uniform density. For geometry *c*, the volume was 24 mL and the density set to 1.0 g mL^{-1}, such that the mass became identical to that of spheres *a* and *b*. This geometry was included to bridge to the calculation of the mean absorbed dose using unit-density sphere S-values described below.

For geometries *a* and *b* and the average absorbed dose rates were calculated using Equations (9) and (10) for varying activity ratios between core and shell. These averages were compared with the mean absorbed dose

for the uniform activity distribution in geometry *c*, and for a 24 g sphere based on the unit-density sphere-model in OLINDA 1.1[22]. S-values were retrieved from the OLINDA program for masses between 0.01 g and 6 kg and a function fitted according to[17]

$$S\ (m) = Am^{-B}, \tag{21}$$

where m is the sphere mass, and A and B are constants whose values were obtained by weighted least-squares fitting using Levenberg-Marquardt's method[39] with the inverse squared S-values as weights.

In addition to averages, the absorbed-dose-rate distributions for geometry *a* were also analyzed as DVHs (Equation 16) and DMHs (Equation 17).

3.3 | Patient examples: Voxel-based tumor dosimetry in treatments with ^{177}Lu-PSMA and ^{177}Lu-DOTA-TATE

The absorbed-dose rate to tumors was calculated for five patients treated with ^{177}Lu-PSMA and six patients treated with ^{177}Lu-DOTA-TATE.

For ^{177}Lu-PSMA, a SPECT/CT image was acquired approximately 100 h (range 94 to 120 h) post administration of 8 GBq (range 7.3 to 8.1 GBq). Three bed positions were used to cover an axial field-of-view from the center of the head down to the thighs, with 60 projection angles per bed position and 30 s per projection in 128 × 128 matrices with 4.42 × 4.42 mm^2 pixel size. A medium-energy collimator and an energy window of 15% centered at 208 keV were employed. Three-dimensional SPECT images were reconstructed using OS-EM with 8 iterations and 6 angles per subset, including compensation for attenuation, scatter using the ESSE method,[40] and distance-dependent spatial resolution. Volumes-of-interest were defined for a total of 162 lesions over all patients by applying an automatic segmentation method based on the difference between Gaussians,[41] and manually removing false positive VOIs over physiologically normal activity uptakes. The density distribution was calculated from the CT by applying a piece-wise linear relationship with two segments between Hounsfield number and density. This relationship was based on previous calibration with a CIRS phantom.[26]

For ^{177}Lu-DOTA-TATE, a SPECT/CT image was acquired approximately 20 h post administration (range 20 to 23 h) of 7.4 GBq (range 7.3 to 7.5 GBq) with a single bed-position over the abdomen. The same settings for acquisition and reconstruction as for PSMA were applied, except that an acquisition time of 45 s per projection was used. Volumes-of-interest were defined for a total of 36 lesions over all patients. Selection and delineation of tumors in SPECT images have been previously described in Roth *et al*.[6]

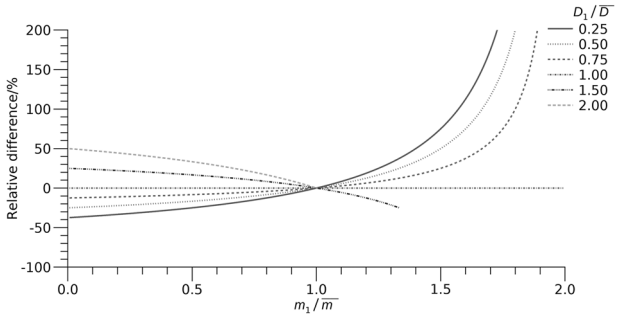

FIGURE 4 Relative difference in the average absorbed dose, $\bar{D}_u/\bar{D} - 1$ (from Equations (4) and (6)), as a function of the mass in region 1 relative to the average mass for regions 1 and 2 (Figure 2). Each colored curve represents the results for a given ratio of the absorbed dose to region 1 and the mean absorbed dose $\bar{D}$ to the two regions, as specified in the legend. Since volumes and absorbed doses are always positive, a given absorbed dose ratio is not compatible with all mass conditions, which is why the curves start and end at different values.

The absorbed-dose rate was calculated on the voxel level using the reconstructed SPECT- and CT-derived activity and density distributions as input to Monte Carlo simulations.[36] Correction for partial volume effects was applied based on recovery coefficients, using previously derived relationships for RC as a function of volume.[6] The mass of each tumor was determined from the density image as the sum of the mass of the voxels within the VOI, calculated as the density multiplied by the voxel volume. The average absorbed dose rate in each tumor was calculated both as the density-weighted region-average (Equation 9) and the region-average (Equation 10). The relative difference $\bar{D}_r/\bar{D} - 1$ was analyzed as function of the density coefficient of variation (CV) within the respective VOI. For comparison, mean absorbed-dose rates were also calculated using mass-derived S-values from Equation (21).

4 | RESULTS

4.1 | Schematic example

Figure 4 shows the relative difference in the average absorbed doses for the geometries in Figure 2, when calculated as $\bar{D}_u$ (Equation 6) or $\bar{D}$ (Equation 4). The ratio $m_1/\bar{m}$ on the abscissa indicates the mass in region 1 in relation to the average mass of the two regions, $\bar{m} = (m_1 + m_2)\ /2$. For the voxels in Figure 2a, the ratio $m_1/\bar{m}$ is identical to the ratio of ρ_1 and the mean density $\bar{\rho} = (m_1 + m_2)\ /(2v)$. For the regions in Figure 2b, the ratio is identical to the ratio of v_1 and the average volume of the two regions, $\bar{v} = (v_1 + v_2)\ /2$. The results are shown for different absorbed doses to region 1 (D_1) relative to $\bar{D}$ calculated according to Equation (6).

The relative difference between the unweighted average $\bar{D}_u$ (Equation 6) and the mass weighted mean $\bar{D}$

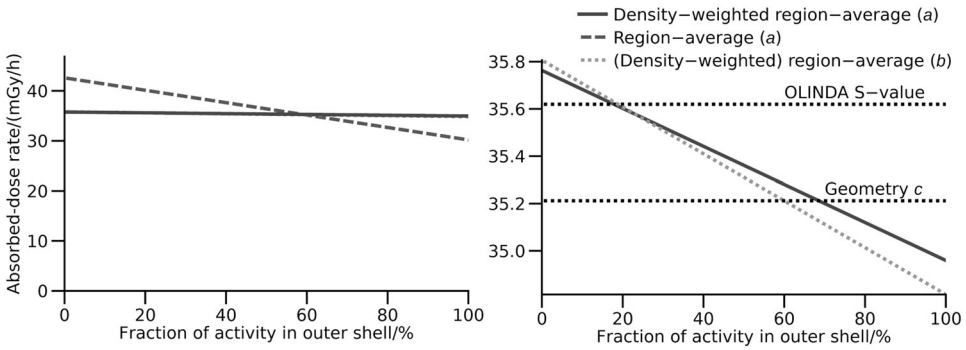

FIGURE 5 Results of different conventions for averaging of absorbed-dose rates in voxel-based dosimetry for geometries *a*, *b*, and *c*, with averages calculated following Equation (9) (density-weighted region average) and 10 (region average). Left panel: Results for geometries *a* and *b* when a variable fraction of the total activity (10 MBq) is in the outer sphere shell. For geometry *b*, with a uniform density, the two averages (Equations (9) and (10)) coincide. Right panel: Resolved differences of the density-weighted average for geometries *a* and *b*, where for comparison, the mean absorbed doses calculated for geometry c and using sphere S-values are included as horizontal dotted lines.

(Equation 4) depends both on the masses of and the absorbed doses to regions 1 and 2. When the masses are equal for two regions, that is, the mass ratio $m_1/\bar{m}$ equals unity, the two averages $\bar{D}_u$ and $\bar{D}$ are equal. Large differences between the unweighted average $\bar{D}_u$ and the mass-weighted average $\bar{D}$ are obtained when there are large differences between m_1 and m_2 (giving small or large mass ratios) and when there is a large difference in total absorbed energy between the regions. For an absorbed-dose ratio $D_1/\bar{D}$ of unity, the two averages $\bar{D}_u$ and $\bar{D}$ are equal.

4.2 | Averaging for voxel-based dosimetry

The density-weighted region-average (Equation 9), the region-average (Equation 10), and the mean absorbed dose calculated with unit-density sphere S-values for the different sphere geometries and varying activity distributions are presented in Figure 5. For geometry *a*, the region-average (Equation 10) gives an average absorbed-dose rate that varies with the fraction of the total sphere activity in the outer shell versus the inner core. The density-weighted region-average changes only marginally across the different distributions, and this form of average is thus insensitive to the distributions of activity and density. Results from the application of S-values and for the uniform sphere in geometry *c* are in-line with the density-weighted region-average. The variation in density-weighted absorbed doses is approximately the same as the difference between the mean absorbed dose for geometry *c* and when using sphere S-values.

Dose-volume- and dose-mass-histograms for different activity distributions in geometry *a* are presented in Figure 6. There are notable differences between DVHs and DMHs, which change depending on the distribution of activity between the inner core and outer shell.

4.3 | Patient examples: Voxel-based tumor dosimetry in treatments with ^{177}Lu-PSMA and ^{177}Lu-DOTA-TATE

The relative differences of the average absorbed-dose rates for the individual tumors were calculated as $\bar{D}_r/\bar{D} - 1$, using the density-weighted region-average $\bar{D}$ (Equation 9) and the region average $\bar{D}_r$ (Equation 10). For ^{177}Lu-PSMA patients (162 tumors in total), the relative difference obtained was (1.1 ± 4.3)% (mean ± SD), with a maximum deviation of +34.4%. For ^{177}Lu-DOTA-TATE patients (36 tumors), the relative difference was (−0.1 ± 0.4)% with a maximum deviation of −1.4%. When considering absorbed-dose rates calculated using sphere S-values (Equation 21), the mean deviation from the density-weighted region average was for ^{177}Lu-PSMA patients (−5.0 ± 1.5)%, with a maximum deviation of −12.3%. For ^{177}Lu-DOTA-TATE patients, the corresponding mean difference was (−2.2 ± 0.9)% with a maximum deviation of −4.4%. The deviations are shown in Figure 7 as function of the within-tumor mass-density CV. The largest deviations between region-averages and density-weighted region-averages were obtained for tumors with a large mass-density CV.

Table 3 shows the averages across tumors on a per-patient basis, calculated using the different conventions for average formation within and between VOIs. Figure 8 shows the corresponding DVHs, DMHs, and DUHs. When taking an unweighted average across the VOI region-averages, the resulting absorbed dose rate was up to 50% lower than when using the density-weighted region-average across the VOIs. Correspondingly, the DUHs were markedly different from the DVHs and DMHs, which in turn had relatively similar shapes. Thus, the largest proportion of the variation in mass between tumors was explained by the different tumor volumes. These differences in average absorbed-dose rate can

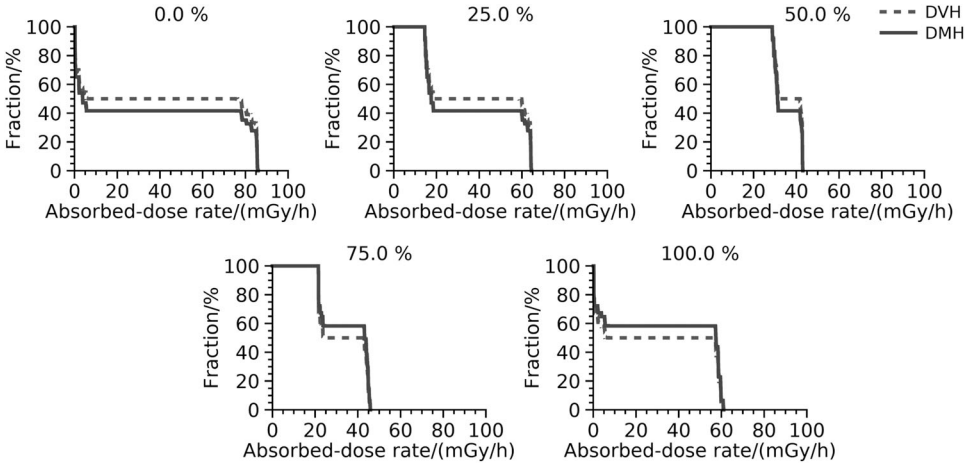

FIGURE 6 Comparison between DMH and DVH for different proportions of the total activity in the outer shell of the sphere.

FIGURE 7 Relative differences in the average absorbed dose for 177Lu-PSMA (a) and 177Lu-DOTA-TATE (b) as function of the coefficient of variation of the density in the respective VOI, used as indicator of the non-uniformity of the density. Filled markers indicate the relative differences between region-averages and density-weighted region-averages from the Monte Carlo simulations and open markers indicate the relative differences between density-weighted region-averages from the Monte Carlo simulation and the mean absorbed doses calculated using S-values. The dashed lines indicate the mean difference and the dotted lines indicate the mean difference ± 1 standard deviation. Examples of maximum-intensity projections of patient SPECT images with projected VOIs indicated are shown for 177Lu-PSMA (c) and 177Lu-DOTA-TATE (d).

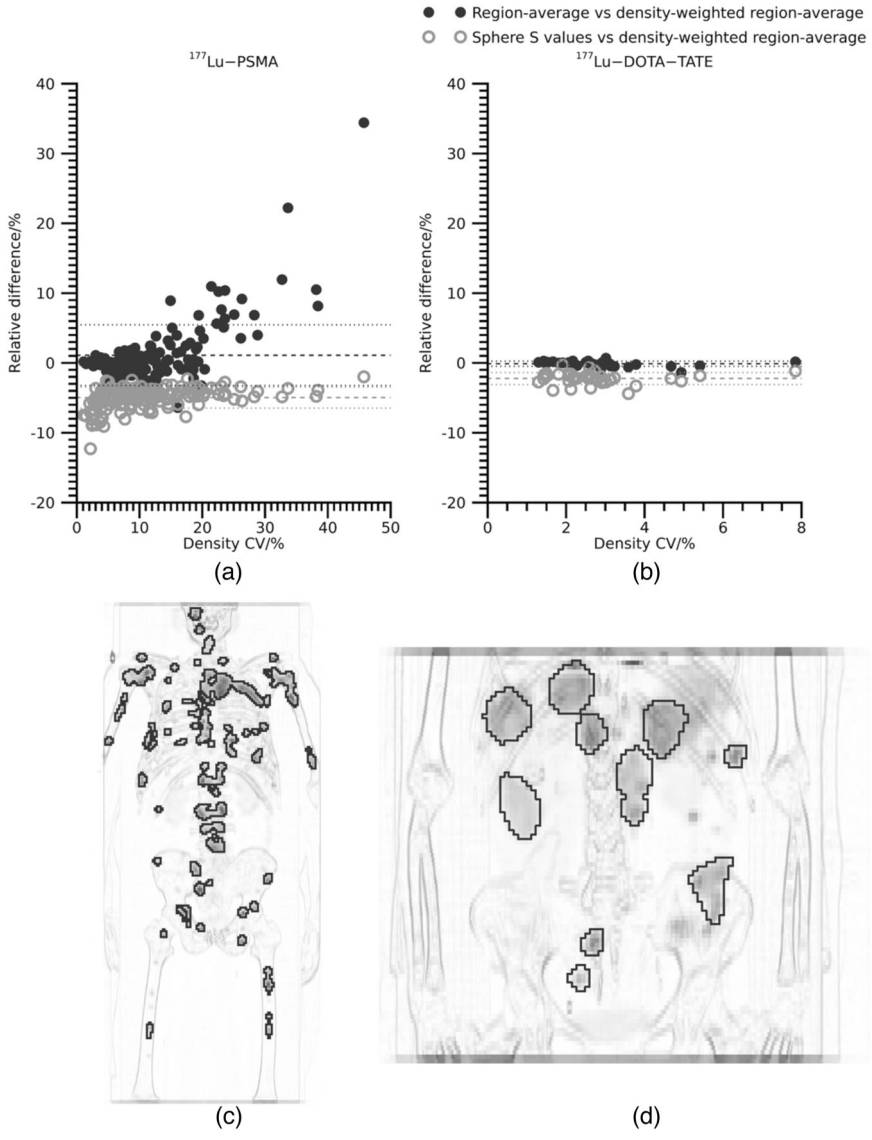

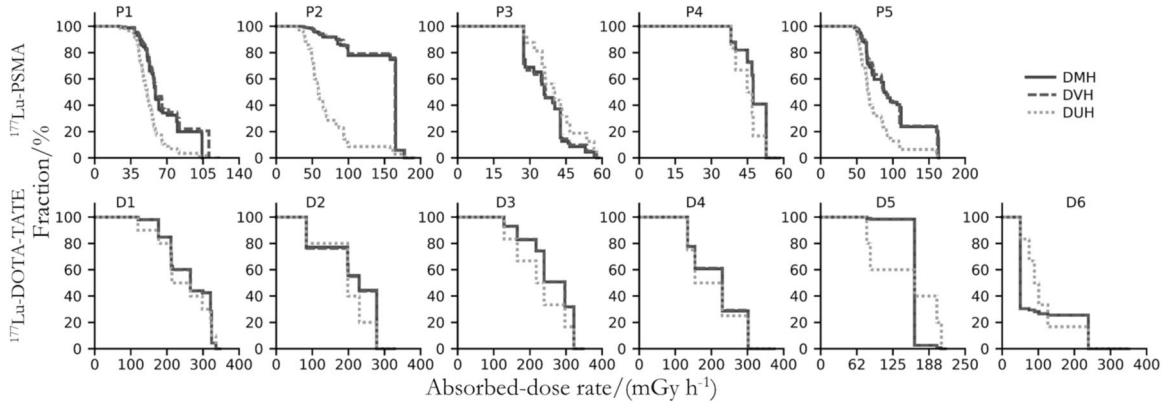

FIGURE 8 Dose-volume histograms (DVHs), dose-mass histograms (DMHs), and unweighted histograms (DUHs) of the absorbed-dose rates for tumor in patients treated with 177Lu-PSMA (upper row) and 177Lu-DOTA-TATE (lower row).

TABLE 3 Average absorbed-dose rates across tumors, calculated using different conventions, for patients treated with ^{177}Lu-PSMA or ^{177}Lu-DOTA-TATE. The averages corresponding to DMHs (Figure 8) are based on density-weighted region averages within the tumors and mass-weighted averages between the tumors. The averages corresponding to DVHs are based on region averages within the tumors and volume-weighted averages between the tumors. For DUHs the averages are based on the region averages within the tumors and unweighted averages between the tumors.

Average absorbed-dose rate/(mGy h^{-1})											
	^{177}Lu-PSMA					^{177}Lu-DOTA-TATE					
Pat. nr	P1	P2	P3	P4	P5	D1	D1	D3	D4	D5	D6
DMH	67	147	37	48	100	263	211	259	217	162	101
DVH	70	147	37	48	101	263	210	260	217	162	100
DUH	53	71	41	45	76	248	198	228	205	148	113

Abbreviations: DMH, dose-mass histogram; DUH, unweighted histogram, DVH, Dose-volume histogram.

be expected to yield similar differences in average absorbed doses.

5 | DISCUSSION

We have shown the importance of differentiating between different forms of averaging of absorbed doses, within regions and between regions. Strategies for absorbed-dose averaging are rarely explicitly addressed in the radiation-physics literature but may in some situations yield substantially different numerical results. It is thus important to be aware which definition for averaging that is applied, and to be explicit when reporting absorbed doses. With respect to comparison studies of dosimetry methods, the same average definition must be used throughout. Otherwise, results may become misleading, with observed deviations reflecting a combination of (relevant) methodological differences and (irrelevant) differences caused by differing average definitions.

For averaging within regions in voxel-based dosimetry, the differences between methods become important when the density distribution is a markedly non-uniform. This is clearly visible in Figure 5, where for geometry *a*, the density-weighted region-average differs from the region-average when the activity distribution changes. The density-weighted region-average gives values that are consistent with geometry *b*, where the density-weighted region-average and the region-average coincide, and where the S-value-based calculations and the uniform sphere in geometry *c* give similar results. Furthermore, as seen in Figure 7 the main differences between the region-average and the density-weighted region-average are obtained for VOIs that have a markedly non-uniform density distribution.

The numerical difference between the results obtained when using different average definitions thus depends on the extent of density variation within the target region. For ^{177}Lu-DOTA-TATE all the studied tumors have modest density variation, and the differences are subtle. For the ^{177}Lu-PSMA cases, some tumors have marked density variation, and the numerical differences are substantial. For example, the tumor with the deviation of 34% in Figure 7a is located in a rib close to the lung interface, making the difference dependent both on the tumor as such and the ability to avoid other tissues in the VOI definition. For the absorbed-dose-rate calculations based on S-values, there are systematic deviations, but with relatively modest variations and without obvious trends as function of density variation within the VOI. The systematic underestimation is a result of the lacking contribution from cross dose, which is not considered in the S-value based calculation. For example, the tumor with a deviation of −12% in Figure 7a has a low uptake of activity but is located close to a large tumor with high activity concentration, making the cross-dose component unusually high relative to the self-dose component.

The density-weighted region-average is consistent with the definition of mean absorbed dose given in ICRU

86[32], and is also equivalent to the mean-absorbed dose calculated according to the MIRD formalism (Equation 13). Thus, the comparison of density-weighted region averages and mean absorbed doses calculated using sphere S-values is a valid method comparison, since these two estimates refer to the same quantity. On the contrary, the comparison of region-averages and density-weighted region-averages is not a valid method comparison, since the two values are not estimates of the same quantity. Under certain conditions, the averages coincide numerically, but their underlying definitions differ. Thus, it is important to distinguish between them.

A hallmark of radionuclide therapy is non-uniform absorbed-dose distributions,[42] both within and between regions, and on a small and macroscopic scale. In clinical dosimetry, the questions arise if and how such non-uniformities should be characterized. A common method is the use of DVHs.[24,43] However, the use of DVHs in clinical dosimetry can be questioned, since the combination of limited spatial resolution and noise in SPECT images leads to heavily distorted histograms in relation to the underlying activity distribution.[44] Drawn to its extreme, it could be argued that the resolution-induced underestimation of the mean activity concentration leads to a substantial error in the first moment (mean) of the absorbed-dose distribution, and it is therefore questionable to calculate higher moments, let alone to try to characterize the distribution as a whole. Several more-or-less advanced methods for partial-volume correction have been proposed, but these typically require the assumption of an underlying uniform activity distribution,[30] and are in principle not compatible with a subsequent characterization of a non-uniformity. A more attainable alternative aim is to characterize the dispersion of absorbed doses between regions. In this study, we describe three different strategies in the form of DMH, DVH, and DUH between regions, representing mass-weighted averages, volume-weighted averages, and unweighted averages (Figure 8 and Table 3). Although the difference between density-weighted region-averages and simple region averages are substantial for individual tumors (Figure 7), the differences between mass-weighted and volume-weighted region-averages values are small in Table 3. However, the unweighted averages give markedly different values. The reason for the largest deviation (patient P2, 147 mGy h^{-1} for DMH and DVH vs. 71 mGy h^{-1} for DUH) was that one large structure, deemed as a single tumor in the segmentation process, comprised 70% of the total tumor burden Thus, it was able to shift the DUH compared with the DMH and DVH (Figure 8), and got a much larger impact when calculating the mass- or volume-weighted averages than when calculating the unweighted average (Table 3).

The intention of this study is not to study radiation transport as such, or how it is affected by density variations. Generally, the radionuclides used for radionuclide therapy emit short-range charged particles, and for ^{177}Lu, more than 80% of the emitted energy is in the form of electrons. In soft tissue and bone, the mean range of the electrons is much shorter than the spatial scale considered in the examples and is also much shorter than the spatial scales that can be resolved with current clinical imaging systems. The emitted electron energy can thus to a good approximation be considered absorbed at the point of decay, meaning that the absorbed-dose rate distribution follows the activity distribution.[44] For a radionuclide where the cross-dose rate component is larger, the results from the Monte-Carlo simulations would be different.

The main foundation for the reasoning in this paper is that ionizing radiation interacts with matter in a region rather than the space occupied by that region. Consequently, from a physics perspective, the density-weighted region-average and mass-weighted average between regions are the most meaningful measures.[32] In the same manner, DMH is a physically more meaningful representation of absorbed-dose non-uniformity than DVH and DUH. At the same time, there are other perspectives, biological and clinical, that need to be considered. For example, if the tolerance absorbed dose for a paired organ at risk has been derived using the unweighted average absorbed dose, then this needs to be considered when applying the associated constraint. Likewise, for multiple tumors in a patient, it is not evident which form of averaging provides the most biologically or clinically meaningful metric.

At reporting of dosimetry results in radionuclide therapy, for research studies, clinical routine, and clinical trials, we find it important to also include information on which strategy was adopted for averaging of absorbed doses, within and between regions. In particular, for commercially available dosimetry programs there is need for transparency in how averages are formed. Preferably, the option to calculate the mean absorbed dose (i.e., a density-weighted region average) should be included, in order to maintain consistency with ICRU concepts[32] and the MIRD formalism. Considering that for most kinds of radionuclide therapies, the absorbed doses that characterize tolerance limits of normal organs and treatment efficacy for tumors are yet to be established, the decision of how absorbed doses are reported is particularly important at this stage. We hope that the current paper supports this development by pointing out the often-overlooked differences between different averaging strategies.

6 | CONCLUSIONS

Characterization of the non-uniformity of absorbed doses within and between regions and averaging of

absorbed dose can be performed in different ways. Different averaging strategies can lead to different dosimetric results, for reasons that are neither related to physics nor to the dosimetry methods used. When comparing methods, and at reporting and recording of absorbed doses, it is important to be aware, and explicit on which averaging strategy is applied, as demonstrated for both stylized geometries and clinical cases. To be consistent with ICRU concepts and the MIRD formalism, the mean absorbed dose (density-weighted region-average) should be used.

ACKNOWLEDGMENTS

This study was financially supported by the Swedish Cancer Society (180747, 211754Pj01H) and Mrs. Berta Kamprad's Foundation (FBKS 2019-44, FBKS-2020-13-293).

CONFLICT OF INTEREST STATEMENT

Sjögreen Gleisner and Ljungberg have participated in research project funded by Fusion Pharmaceuticals Inc., Canada. Sjögreen Gleisner has acted as consultant for Spago Nanomedical.

DATA AVAILABILITY STATEMENT

Authors will share data upon request to the corresponding author.

REFERENCES

1. Strigari L, Konijnenberg M, Chiesa C, et al. The evidence base for the use of internal dosimetry in the clinical practice of molecular radiotherapy. *Eur J Nucl Med Mol I*. 2014;41:1976-1988.
2. Barone R, Borson-Chazot FO, Valkerna R, et al. Patient-specific Dosimetry in predicting renal toxicity with ^{90}Y-DOTATOC: relevance of kidney volume and dose rate in finding a dose-effect relationship. *J Nucl Med*. 2005;46:99s-106s.
3. Ilan E, Sandström M, Wassberg C, et al. Dose response of pancreatic neuroendocrine tumors treated with peptide receptor radionuclide therapy using ^{177}Lu-DOTATATE. *J Nucl Med*. 2015;56:177-182.
4. Pauwels S, Barone R, Walrand S, et al. Practical dosimetry of peptide receptor radionuclide therapy with ^{90}Y-labeled somatostatin analogs. *J Nucl Med*. 2005;46:92s-98s.
5. Hagmarker L, Svensson J, Ryden T, et al. Bone marrow absorbed doses and correlations with hematologic response during ^{177}Lu-DOTATATE treatments are influenced by image-based dosimetry method and presence of skeletal metastases. *J Nucl Med*. 2019;60:1406-1413.
6. Roth D, Gustafsson J, Warfvinge CF, et al. Dosimetric quantities in neuroendocrine tumors over treatment cycles with ^{177}Lu-DOTATATE. *J Nucl Med*. 2022;63:399-405.
7. Sundlöv A, Sjögreen Gleisner K, Tennvall J, et al. Phase II trial demonstrates the efficacy and safety of individualized, dosimetry-based ^{177}Lu-DOTATATE treatment of NET patients. *Eur J Nucl Med Mol I*. 2022;49:3830-3840.
8. Finocchiaro D, Berenato S, Bertolini V, et al. Comparison of different calculation techniques for absorbed dose assessment in patient specific peptide receptor radionuclide therapy. *Plos One*. 2020;15:e0236466.
9. Götz T, Schmidkonz C, Lang EW, Maier A, Kuwert T, Ritt P. A comparison of methods for adapting ^{177}Lu dose-voxel-kernels to tissue inhomogeneities. *Phys Med Biol*. 2019;64:245011.
10. Grassi E, Fioroni F, Ferri V, et al. Quantitative comparison between the commercial software STRATOS® by Philips and a homemade software for voxel-dosimetry in radiopeptide therapy. *Phys Medica*. 2015;31:72-79.
11. Grimes J, Celler A. Comparison of internal dose estimates obtained using organ-level, voxel S value, and Monte Carlo techniques. *Med Phys*. 2014;41:092501.
12. Mikell JK, Mahvash A, Siman W, Mourtada F, Kappadath SC. Comparing voxel-based absorbed dosimetry methods in tumors, liver, lung, and at the liver-lung interface for ^{90}Y microsphere selective internal radiation therapy. *Ejnmmi Phys*. 2015;2:16.
13. Brosch-Lenz J, Uribe C, Gosewisch A, et al. Influence of dosimetry method on bone lesion absorbed dose estimates in PSMA therapy: application to mCRPC patients receiving Lu-177-PSMA-I&T. *Ejnmmi Phys*. 2021;8:26.
14. Sgouros G, Bolch WE, Chiti A, et al. ICRU Report 96, dosimetry-guided radiopharmaceutical therapy. *J ICRU*. 2021;21:1-212.
15. International Atomic Energy Agency. Dosimetry for Radiopharmaceutical Therapy [IAEA preprint]. preprint.iaea.org/search.aspx?orig_q=RN:53037189 2022.
16. Bartlett RM, Bolch WE, Brill AB, et al. *MIRD Primer 2022: A Complete Guide to Radiopharmaceutical Dosimetry*. Society of Nuclear Medicine & Molecular Imaging; 2022.
17. Gear JI, Cox MG, Gustafsson J, et al. EANM practical guidance on uncertainty analysis for molecular radiotherapy absorbed dose calculations. *Eur J Nucl Med Mol I*. 2018;45:2456-2474.
18. Gustafsson J, Brolin G, Cox M, Ljungberg M, Johansson L, Sjögreen Gleisner K. Uncertainty propagation for SPECT/CT-based renal dosimetry in ^{177}Lu peptide receptor radionuclide therapy. *Phys Med Biol*. 2015;60:8329-8346. doi: 10.1088/0031-9155/60/21/8329
19. Bolch WE, Eckerman KF, Sgouros G, Thomas SR. MIRD pamphlet no. 21: a generalized schema for radiopharmaceutical dosimetry - standardization of nomenclature. *J Nucl Med*. 2009;50:477-484.
20. Andersson M, Johansson L, Eckerman K, Mattsson S. IDAC-Dose 2.1, an internal dosimetry program for diagnostic nuclear medicine based on the ICRP adult reference voxel phantoms. *Ejnmmi Res*. 2017;7:88.
21. Chauvin M, Borys D, Botta F, et al. OpenDose: open-access resource for nuclear medicine dosimetry. *J Nucl Med*. 2020;61:1514-1519.
22. Stabin MG, Sparks RB, Crowe E. OLINDA/EXM: The second-generation personal computer software for internal dose assessment in nuclear medicine. *J Nucl Med*. 2005;46:1023-1027.
23. Bolch WE, Bouchet LG, Robertson JS, et al. MIRD pamphlet No. 17: the dosimetry of nonuniform activity distributions - Radionuclide S values at the voxel level. *J Nucl Med*. 1999;40:11S-36S.
24. Chiesa C, Mira M, Maccauro M, et al. Radioembolization of hepatocarcinoma with ^{90}Y glass microspheres: development of an individualized treatment planning strategy based on dosimetry and radiobiology. *Eur J Nucl Med Mol I*. 2015;42:1718-1738.
25. Schneider W, Bortfeld T, Schlegel W. Correlation between CT numbers and tissue parameters needed for Monte Carlo simulations of clinical dose distributions. *Phys Med Biol*. 2000;45:459-478.
26. Sjögreen-Gleisner K, Rueckert D, Ljungberg M. Registration of serial SPECT/CT images for three-dimensional dosimetry in radionuclide therapy. *Phys Med Biol*. 2009;54:6181-6200.
27. Dieudonné A, Hobbs RF, Lebtahi R, et al. Study of the impact of tissue density heterogeneities on 3-dimensional abdominal dosimetry: comparison between dose kernel convolution and direct monte carlo methods. *J Nucl Med*. 2013;54:236-243.

28. Sundlöv A, Sjögreen-Gleisner K, Svensson J, et al. Individualised ^{177}Lu-DOTATATE treatment of neuroendocrine tumours based on kidney dosimetry. *Eur J Nucl Med Mol I*. 2017;44:1480-1489.
29. Violet J, Jackson P, Ferdinandus J, et al. Dosimetry of ^{177}Lu-PSMA-617 in metastatic castration-resistant prostate cancer: correlations between pretherapeutic imaging and whole-body tumor dosimetry with treatment outcomes. *J Nucl Med*. 2019;60:517-523.
30. Erlandsson K, Buvat I, Pretorius PH, Thomas BA, Hutton BF. A review of partial volume correction techniques for emission tomography and their applications in neurology, cardiology and oncology. *Phys Med Biol*. 2012;57:R119-R159.
31. Seltzer SM, Bartlett DT, Burns DT, et al. ICRU report no. 85: fundamental quantities and units for ionizing radiation (revised). *J ICRU*. 2011;11(1):1-31.
32. Braby LA, Brooks AL, Heidenreich WF, et al. ICRU report no. 86: quantification and reporting of low-dose and other heterogeneous exposures. *J ICRU*. 2011;11(2):1-77.
33. Shannon CE. Communication in the presence of noise. *P Ire*. 1949;37:10-21.
34. Herman GT, Lent A. Iterative reconstruction algorithms. *Comput Biol Med*. 1976;6:273-294.
35. Nioutsikou E, Webb S, Panakis N, Bortfeld T, Oelfke U. Reconsidering the definition of a dose-volume histogram. *Phys Med Biol*. 2005;50:L17-L19.
36. Ljungberg M, Sjögreen K, Liu X, Frey E, Dewaraja Y, Strand S-E. A 3-dimensional absorbed dose calculation method based on quantitative SPECT for radionuclide therapy: evaluation for ^{131}I using Monte Carlo simulation. *J Nucl Med*. 2002;43:1101-1109.
37. Kawrakow I. Accurate condensed history Monte Carlo simulation of electron transport. I. EGSnrc, the new EGS4 version. *Med Phys*. 2000;27:485-498.
38. Bé M-M, Chisté V, Dulieu C, et al. *Monographie BIPM-5 Table of Radionuclides*. Bureau international des Poids et Mesures; 2004.
39. Markwardt CB. Non-linear Least-squares Fitting in IDL with MPFIT. 2009:251-254.
40. Frey EC, Tsui BMW. A new method for modeling the spatially-variant, object-dependent scatter response function in SPECT. *Ieee Nucl Sci Conf R*. 1997:1082-1086.
41. Sjögreen Gleisner K, Gustafsson J, Stenvall A, et al. Estimation of tumor burden from ^{68}Ga- Dotatate-PET/CT and day-7 planar ^{177}Lu images, for patients treated with ^{177}Lu-Dotatate. *Eur J Nucl Med Mol Imaging*. 2020;47(Suppl 1):5376.
42. Konijnenberg M, Melis M, Valkema R, Krenning E, de Jong M. Radiation dose distribution in human kidneys by octreotides in peptide receptor radionuclide therapy. *J Nucl Med*. Jan 2007;48:134-142.
43. Prideaux AR, Song H, Hobbs RF, et al. Three-dimensional radiobiologic dosimetry: application of radiobiologic modeling to patient-specific 3-dimensional imaging-based internal dosimetry. *J Nucl Med*. 2007;48:1008-1016.
44. Ljungberg M, Sjögreen-Gleisner K. The accuracy of absorbed dose estimates in tumours determined by quantitative SPECT: a Monte Carlo study. *Acta Oncol*. 2011;50:981-989.

How to cite this article: Gustafsson J, Ljungberg M, Alm Carlsson G, et al. Averaging of absorbed doses: How matter matters. *Med Phys*. 2023;50:6600–6613.
https://doi.org/10.1002/mp.16528

APPENDIX A

Consider two regions with masses m_1 and m_2 and mean absorbed doses D_1 and D_2 (Equation 2). The average mass of the two regions is

$$\bar{m} = \frac{m_1 + m_2}{2}, \tag{A1}$$

the density-weighted region average absorbed dose follows from Equation (4), according to

$$\bar{D} = \frac{D_1 m_1 + D_2 m_2}{m_1 + m_2}, \tag{A2}$$

and the unweighted average absorbed dose is

$$\bar{D}_u = \frac{D_1 + D_2}{2}. \tag{A3}$$

The ratio $\bar{D}_u/\bar{D}$ becomes

$$\begin{aligned}\frac{\bar{D}_u}{\bar{D}} = \frac{D_1 + D_2}{2\bar{D}} &= \frac{D_1(2\bar{m} - m_1) + 2\bar{D}\bar{m} - D_1 m_1}{2\bar{D}(2\bar{m} - m_1)} \\ &= \frac{1}{2}\frac{D_1}{\bar{D}}\frac{2\bar{m} - m_1 + 2\bar{m}\bar{D}/\bar{D}_1 - m_1}{2\bar{m} - m_1} \\ &= \frac{1}{2}\alpha\left(1 + \frac{2\alpha^{-1} - \beta}{2 - \beta}\right),\end{aligned} \tag{A4}$$

where $\alpha = \bar{D}_1/\bar{D}$ and $\beta = \bar{m}_1/\bar{m}$.

The fact that $m_1 > 0$ and $m_2 > 0$ gives

$$0 < \beta < 2, \tag{A5}$$

and in combination with $D_1 \geq 0$ and $D_2 \geq 0$ also

$$0 \leq \alpha \leq \frac{m_1 + m_2}{m_1} = 2\beta^{-1}. \tag{A6}$$